Circular-Polarization-Dependent Study of Microwave-Induced Conductivity Oscillations in a Two-Dimensional Electron Gas on Liquid Helium

Circular-Polarization-Dependent Study of Microwave-Induced Conductivity Oscillations in a Two-Dimensional Electron Gas on Liquid Helium

A. A. Zadorozhko,[1] Yu. P. Monarkha,[2] and D. Konstantinov[1,*]
[1]Quantum Dynamics Unit, Okinawa Institute of Science and Technology, Tancha 1919-1, Okinawa 904-0495, Japan
[2]Institute for Low Temperature Physics and Engineering, 47 Nauky Avenue, 61103 Kharkiv, Ukraine

(Received 2 October 2017; published 26 January 2018)

The polarization dependence of the photoconductivity response at cyclotron-resonance harmonics in a nondegenerate two-dimensional (2D) electron system formed on the surface of liquid helium is studied using a setup in which a circular polarization of opposite directions can be produced. Contrary to the results of similar investigations reported for semiconductor 2D electron systems, for electrons on liquid helium, a strong dependence of the amplitude of magnetoconductivity oscillations on the direction of circular polarization is observed. This observation is in accordance with theoretical models based on photon-assisted scattering, and, therefore, it presents a principal argument in the dispute over the origin of microwave-induced conductivity oscillations.

DOI: 10.1103/PhysRevLett.120.046802

Studies of microwave (MW) photoconductivity in a two-dimensional (2D) electron gas of semiconductor heterostructures (GaAs/AlGaAs) subjected to a perpendicular magnetic field B have revealed remarkable magnetotransport phenomena: giant microwave-induced resistance oscillations (MIROs) [1,2] and associated zero resistance states [3,4]. These discoveries have opened a prominent research area and triggered a large body of theoretical works. The universality of the effect of MIROs was proved by similar observations in hole systems [5], MgZnO/ZnO heterostructures [6], and a nondegenerate 2D electron system formed on the free surface of liquid helium [7].

It is very surprising that by now there is a great body of different theoretical mechanisms explaining MIROs which use quantum and classical effects (for a review, see [8]), but the origin of these oscillations is still under debate. Among these mechanisms, there is a large group of models whose description is based on the concept of the photon-assisted scattering off disorder which overcomes the selection rules existing for direct photon-induced transitions; direct transitions can be only between adjacent Landau levels: $n' - n = \pm 1$. The photon-assisted scattering leads to two important effects. First, it gives a separate contribution to magnetoconductivity σ_{xx} where the displacement of the electron orbit center $X' - X$ caused by energy conservation changes its sign when the ratio ω/ω_c passes an integer $m = n' - n = 1, 2, \ldots$ (here ω is the MW frequency and ω_c is the cyclotron frequency) [9,10]. This mechanism is called the displacement model (DM).

Second, electron scattering to higher Landau levels ($n' - n = 2, 3, \ldots$) changes the distribution function of electrons at these levels $f(\varepsilon)$: It acquires an oscillatory form with maxima, and, therefore, a sort of population inversion occurs [11,12]. This mechanism is called the inelastic model (IM), because the inelastic thermalization rate is an important quantity for the description of the effect. The maxima of $f(\varepsilon)$ affect the contribution to σ_{xx} caused by usual scattering processes and also lead to a sign-changing correction to σ_{xx}.

Both theoretical models (DM and IM) give satisfactory descriptions of MIROs in semiconductor electron systems. Still, there is a critical unresolved issue which concerns the dependence of MIROs on the direction of circular polarization: The results of the DM and IM are very sensitive to the direction of circular polarization, while the MIROs observed in semiconductor heterostructures are notably immune to the sense of circular polarization [13] or have a very weak dependence on the direction of circular polarizations in the terahertz range [14] which is at odds with existing theories of MIROs.

The theoretical analysis [15] of the DM and IM performed for a nondegenerate 2D electron gas on liquid helium also indicates that both models result in practically the same strong dependence of the amplitude of MIROs on the direction of circular polarization if the number $m = 2, 3, \ldots$ is not large. Since the MIROs observed for electrons on liquid helium [7] are in good accordance with the IM, and the recent observation of MW-induced oscillations in magnetocapacitance of a semiconductor system [16] also supports the concept of a nonequilibrium distribution function oscillating with energy, there is a strong need to investigate the dependence of the amplitude of magnetoconductivity oscillations on the direction of circular polarization for the 2D electron system on liquid helium.

In this Letter, we report the first observation of a strong dependence of the amplitude of microwave-induced magnetoconductivity oscillations on the direction of circular

polarization in the electrons-on-helium system. The analysis of data given here shows that this observation is in accordance with theoretical models based on photon-assisted scattering. Thus, contrary to the mysterious contradiction between experiment and theory existing in semiconductor heterostructures, the circular-polarization-dependent study of MIRO in a nondegenerate 2D electron gas on liquid helium provides strong support for photon-assisted scattering as the origin of the magnetoconductivity oscillations.

The experiments are done in a 2D electron system formed on the free surface of liquid ^{3}He, which is contained in a closed cylindrical cell and cooled to $T = 0.2$ K. At this temperature, the scattering of electrons is dominated by capillary-wave excitations of the liquid helium surface (ripplons) and is very well understood [17,18]. The magnetic field B is applied perpendicular to the liquid surface, and the longitudinal conductivity of electrons σ_{xx} is measured by the capacitive-coupling method using a pair of gold-plated concentric circular electrodes (Corbino disk) placed beneath and parallel to the liquid surface. The electrodes have outer diameters of 14 and 19.8 mm and are separated by a gap of width 0.005 mm. Similar to our previous experiment [7], conductivity oscillations are excited by the electric field component of the fundamental TEM_{002} mode in a semi-confocal Fabry-Pérot resonator [19]. The resonator is formed by the Corbino disk acting as a flat reflecting mirror and a copper concave (radius of curvature 30 mm) mirror of diameter 35.2 mm placed above and parallel to the Corbino disk at a distance about 13 mm. At liquid helium temperatures, the TEM_{002} mode has a frequency $\omega_r/2\pi \approx 35.21$ GHz, and the quality factor is about 10^4.

The MW excitation is supplied from a room-temperature source followed by a linear-to-circular polarization converter, transmitted into the cryostat via a circular (inner diameter 6.25 mm) 1.5-m-long waveguide, and then coupled to the resonator via a circular aperture (diameter 1.8 mm) drilled in the center of the concave mirror. The axial symmetry and alignment of this setup are very important to ensure the circular polarization of the resonant mode field excited in the resonator. To check the latter, we observed the dependence of the cyclotron resonance (CR) excited in a 2D electron system by the circular-polarized MWs on the direction of the applied magnetic field. For this, the electrons were placed in the maximum of the MW E field in the resonator by adjusting the height of the liquid helium to be about 2.1 mm above the Corbino disk, and the value of the magnetic field B was adjusted such that the cyclotron frequency of electrons, $\omega_c = eB/m_e c$, was close to the frequency of the resonant mode.

To detect the photoconductivity response of electrons, we applied a 20 mV excitation voltage at the frequency of 1.117 kHz to the inner electrode of the Corbino disk and measured the current induced in the outer electrode by the electron motion. This current is plotted in Fig. 1 as a function

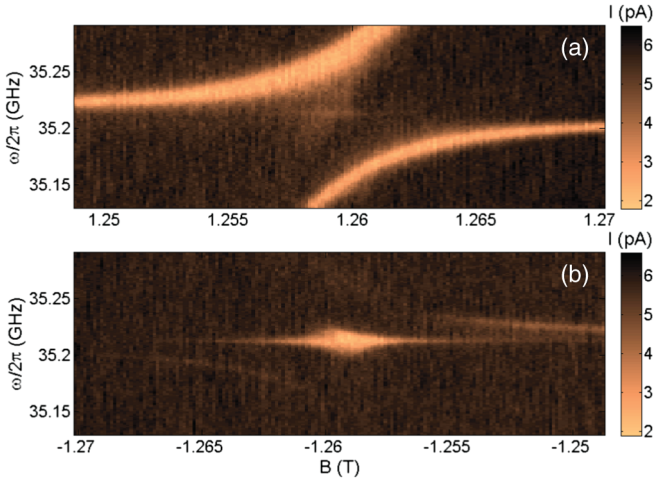

FIG. 1. Photocurrent response of the 2D electron system at $T = 0.2$ K and electron density $n_s = 8.2 \times 10^7$ cm^{-2} to a circular-polarized microwave excitation plotted as a function of MW frequency ω and perpendicular magnetic field B. Panels (a) and (b) are for two opposite directions of the field distinguished by the sign of B.

of the magnetic field B and the frequency of MW excitation ω. Two panels correspond to two opposite directions of the magnetic field B. For a given direction of circular polarization, strong CR absorption should occur only for the proper direction of the magnetic field and should be strongly suppressed for the opposite direction. As was demonstrated earlier [20], for a resonator of a sufficiently high quality factor, the strong coupling of cyclotron motion of electrons to the resonator mode leads to the appearance of two polaritonic branches of coupled electron-mode motion. This is shown in Fig. 1(a), where two polaritonic branches are revealed in the conductivity response of electrons due to their strong heating by the CR absorption. For the opposite direction of the magnetic field [see Fig. 1(b)], the polaritonic branches are barely visible, pointing out that the CR absorption is strongly suppressed. The origin of a strong response appearing around the crossover point $\omega_r = \omega_c$, which corresponds to $B \approx 1.26$ T, is not clear. For the opposite direction of circular polarization, the polaritonic branches are clearly observed for negative B and are strongly suppressed for positive B. Finally, for linear polarized MWs, polaritonic branches of nearly equal intensity are observed for both directions of the field B.

Next, we consider the photoconductivity response of electrons at the harmonics of the CR by varying the value of B in a wide range for both directions of the field. Figure 2(a) shows the current signal measured at $T = 0.2$ K for MW excitation which is circularly polarized in the same direction as for the data shown in Fig. 1. A strong photocurrent response is observed near values of B which satisfy the condition $\omega = m\omega_c$, where $m = 2, 3, \ldots$. In addition, the photocurrent response is observed only when the frequency of microwave excitation ω is in the

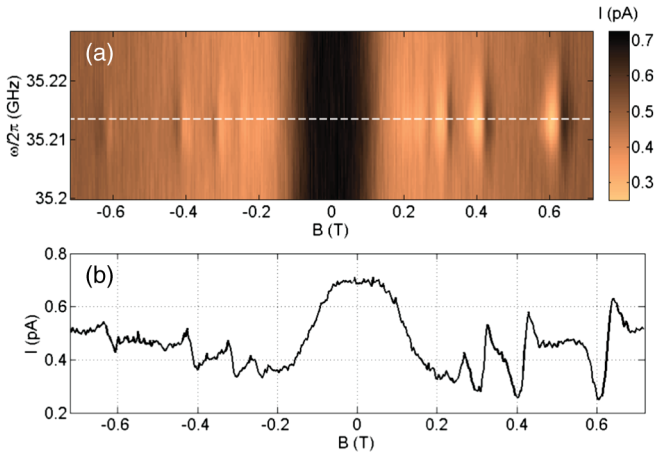

FIG. 2. (a) Photocurrent response of the 2D electron system at $T = 0.2$ K and electron density $n_s = 5.2 \times 10^6$ cm^{-2} to circular-polarized MWs plotted as a function of MW frequency ω and perpendicular magnetic field B. (b) Photocurrent response taken at $\omega = \omega_r$ [indicated by a dashed line in panel (a)].

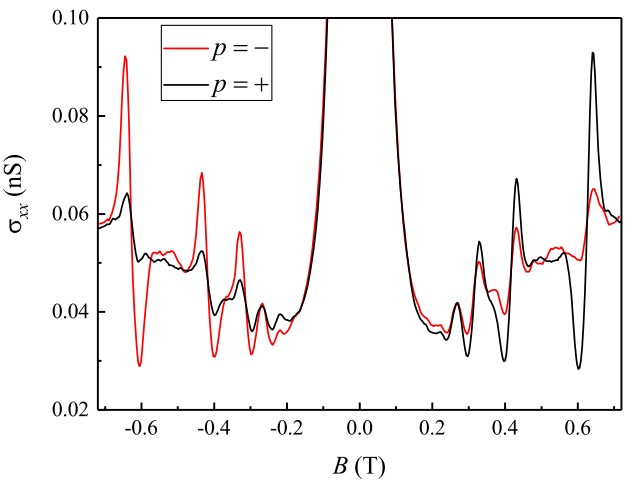

FIG. 3. Longitudinal conductivity σ_{xx} of 2D electrons at $T = 0.2$ K and $n_s = 5.1 \times 10^6$ cm^{-2} versus magnetic field B for two directions of circular polarization of MWs at frequency $\omega/2\pi = 35.213$ GHz. A black line is for the circular polarization direction ($p = +$) the same as for data shown in Figs. 1 and 2, while a red line is for the opposite direction ($p = -$).

vicinity of the resonant frequency ω_r. In particular, Fig. 2(b) displays the current signal measured at $\omega = \omega_r$. As shown previously [7], the photoconductivity oscillations can be observed only when the amplitude of the microwave E field is sufficiently large, which occurs near the cavity resonance. For the input MW power used in Fig. 2, we crudely estimate a maximum amplitude of the E field in the resonant TEM_{002} mode of about 5 V/cm.

The most important feature of plots shown in Figs. 2(a) and 2(b) is a significant asymmetry in the amplitude of the photocurrent response with respect to the directions of B. In particular, the large current oscillations are observed in the direction of the B field corresponding to strong CR absorption, while the oscillations are strongly reduced for the direction of the field corresponding to suppressed CR absorption; cf. Figs. 1(a) and 1(b). For the opposite direction of circular polarization (data not shown), the situation is reversed with respect to the direction of B, which is consistent with the behavior of CR absorption described above. Finally, for linear polarized microwaves, the amplitude of oscillations was found to be the same for both directions of B.

Figure 3 shows values of σ_{xx} extracted from the measured current signals and plotted as a function of the magnetic field B for two opposite directions of circular polarization. The strong dependence of the amplitude of oscillations on the direction of circular polarization indicated in Fig. 3 is the central result of this work and is at least in qualitative agreement with predictions of the theories based on photon-assisted scattering. For the sake of a quantitative comparison, we consider theoretical predictions with some more details below.

To obtain probabilities of photon-assisted scattering, there is a nonperturbative treatment resulting in the Landau-Floquet states which includes the MW field in an exact form (for recent examples, see [15,21–23]). The wave function of these states has a time-dependent shift of the center position $\xi(t)$ and a special phase factor. Considering two components of the MW field $E^{(x)} = a_p E_{\mathrm{MW}} \cos \omega t$ and $E^{(y)} = b_p E_{\mathrm{MW}} \sin \omega t$ (here the numbers a_p and b_p describe the MW polarization, and p is the polarization index), one has to introduce two time-dependent shifts ξ (along the x axis) and ζ (along the y axis), which satisfy classical equations of motion [15]. The important consequence of this treatment is that the new expression for the matrix elements $\langle n', X'|e^{-i\mathbf{q}\cdot\mathbf{r}}|n, X\rangle_{L-F}$ describing electron scattering off disorder acquires an additional exponential factor

$$\exp\left[-i\beta_{p,\mathbf{q}} \sin\left(\omega t + \gamma_p\right)\right], \tag{1}$$

as compared to the conventional form obtained for the Landau basis. Here

$$\beta_{p,\mathbf{q}} = \lambda \omega_c l_B \frac{\sqrt{q_y^2(a_p\omega_c + b_p\omega)^2 + q_x^2(a_p\omega + b_p\omega_c)^2}}{(\omega^2 - \omega_c^2)}, \tag{2}$$

$\lambda = eE_{\mathrm{MW}} l_B/\hbar\omega$ is the parameter describing the strength of the MW field, $l_B^2 = \hbar c/eB$, and the exact form of γ_p is not important for the following discussion.

The calculation of scattering probabilities is reduced to the usual treatment by means of the Jacobi-Anger expansion $e^{iz\sin\phi} = \sum_k J_k(z)e^{ik\phi}$ [here $J_k(z)$ is the Bessel function]. Thus, the probability of one-photon-assisted scattering is proportional to $J_1^2(\beta_{p,\mathbf{q}}) \simeq \beta_{p,\mathbf{q}}^2/4$, if the parameter $\beta_{p,\mathbf{q}}$ is small. Therefore, the ratio of MW-induced

corrections to the dc dissipative conductivity obtained for different directions of circular polarization ($p = +$ and $p = -$; $a_\pm = 1$, $b_\pm = \pm 1$) is described by the simple relationship

$$\frac{\Delta\sigma_{xx}^{(+)}}{\Delta\sigma_{xx}^{(-)}} = \frac{(\omega/\omega_c + 1)^2}{(\omega/\omega_c - 1)^2}. \tag{3}$$

This equation is valid for the both DM and IM, because $\beta_{p,\mathbf{q}}$ is now independent of the direction of the wave vector $\mathbf{q}$. The ratio of Eq. (3) is large for $m = 2$ (it equals 9) and $m = 3$ (it equals 4), but it approaches unity if m increases. Calculations based on Eq. (2) indicate that deviations from circularity (elliptic polarization) can reduce the ratio $\Delta\sigma_{xx}^{(+)}/\Delta\sigma_{xx}^{(-)}$.

Equation (3) follows from the Landau-Floquet states and equations of motion for $\xi(t)$ and $\zeta(t)$ which naturally do not include any damping. A similar equation for the ratio of the oscillation amplitudes found in a different way [14] contains an additional dimensionless parameter proportional to n_s: the superradiant decay rate. For electrons on liquid helium, this parameter is extremely small because of low electron densities (here $n_s \simeq 5 \times 10^6$ cm^{-2}) and the free electron mass. It should be noted also that, for surface electrons, typical damping parameters (level broadening and momentum relaxation rate) are dominated by electron-ripplon scattering, and usually they are much smaller than ω_c. The special case $\omega_c \to \omega$ is not considered here because of the huge heating of electrons and an instability occurring at $B > 1.1$ T.

For both the DM and IM, the shape of MIROs was shown to be similar to experimental observations [7,15]. Therefore, here we concentrate on the comparison of polarization dependencies of MIROs. The ratio of the amplitudes of conductivity oscillations obtained here for two opposite directions of circular polarization is illustrated in Fig. 4. The amplitudes of oscillations were extracted from conductivity data by removing the average background of a respective curve which was approximately extended in the region of oscillatory variations. The experimental results were plotted separately for maxima (solid circles and squares) and minima (open circles and squares), because the ratio of Eq. (3) shown in this figure by the solid curve depends strongly on B. The accuracy of this procedure is confirmed by the ratio of peak-to-peak amplitudes (triangles) which does not depend on the background. To fix positions of the peak-to-peak ratio on the B axis, we used positions of nodes at harmonics of the CR. To ensure that a possible power difference did not affect our results here, we plotted (squares and crosses) the ratio of respective amplitudes obtained at positive and negative B from the same curve of Fig. 3.

Figure 4 indicates that the ratio $\Delta\sigma_{xx}^{(+)}/\Delta\sigma_{xx}^{(-)}$ found in the experiment increases with lowering ω/ω_c in accordance

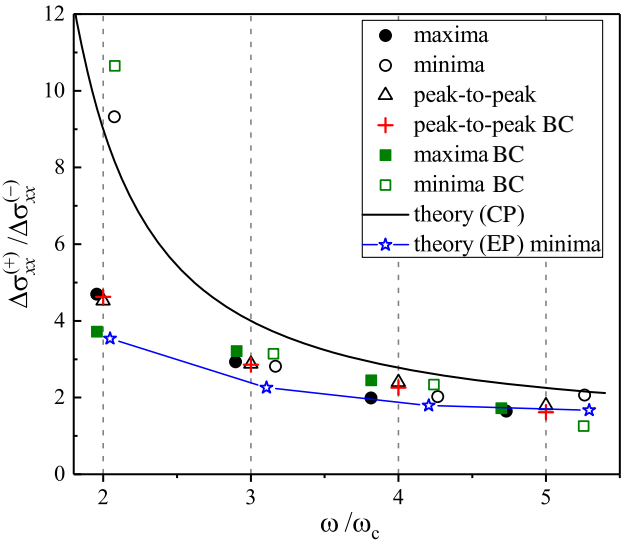

FIG. 4. The ratio $\Delta\sigma_{xx}^{(+)}/\Delta\sigma_{xx}^{(-)}$ versus ω/ω_c: Results obtained from experimental data for conductivity maxima (solid circles and squares) and minima (open circles and squares), the ratio of peak-to-peak amplitudes (triangles and crosses), and the ratio of amplitudes obtained for positive and negative B using the black curve (BC) of Fig. 3, theory [Eq. (3)] calculated for the circular polarization (CP, solid curve), and theory using the elliptic polarization (EP) with $a_\pm = 0.7$ and $b_\pm = \pm 1.3$ calculated for minima (open stars).

with the theory; still, it at an average is lower than theoretical values by a factor of the order of unity (about 1.4). As a possible reason for such a reduction, we considered a deviation from circularity. By way of illustration, calculations employing the DM and Eq. (2) with $a_\pm = 0.7$ and $b_\pm = \pm 1.3$ are shown in Fig. 4 by star symbols with lines. Actually, the chosen parameters of ellipticity give an even stronger reduction of the ratio $\Delta\sigma_{xx}^{(+)}/\Delta\sigma_{xx}^{(-)}$ than that observed in the experiment. It should be noted that the chosen ellipticity still leads to a strong suppression (about 10 times) of the photocurrent response at CR conditions for MWs with $p = -$, which is consistent with observations shown in Fig. 1. For inverted parameters ($a_\pm = 1.3$, $b_\pm = \pm 0.7$), the reduction of the ratio of amplitudes is less than 5%, because the integrand of the conductivity equation contains the symmetry-breaking factor q_y^2. Since the Corbino experiment gives σ_{xx} data averaged over all directions of the driving electric field, the actual reduction of the ratio $\Delta\sigma_{xx}^{(+)}/\Delta\sigma_{xx}^{(-)}$ for $a_\pm = 0.7$ and $b_\pm = \pm 1.3$ can be noticeably less than that shown in Fig. 4 by star symbols.

Under the conditions of the experiment, the average Coulomb interaction energy per electron is more than 30 times larger than the average kinetic energy (temperature). A significant part of this interaction is taken into account [15] using a model of a quasiuniform electric field of fluctuational origin [24]. Still, a small nonuniform part of the fluctuational electric field can affect the model used for obtaining Eqs. (2) and (3). Additionally, one cannot

completely exclude the heating of surface electrons by MWs. Therefore, the agreement between the experiment and the theories based on photon-assisted scattering can be considered as satisfactory.

At $E_{MW} = 5\mathrm{V/cm}$, both the DM and IM are estimated to provide sufficient amplitudes of MIROs under the conditions of this experiment, but the circular-polarization study cannot determine the contribution of which model dominates. For liquid ^{3}He, there is also an uncertainty in the definition of the inelastic thermalization rate, because short wavelength ripplons responsible for interlevel scattering are heavily damped at low temperatures. Assuming that we can still rely on the usual ripplon spectrum, the IM yields somewhat stronger amplitudes of MIROs than the DM. Still, for a strict conclusion, an experimental setup with different linear polarizations and a fixed direction of the dc field is required.

Figures 3 and 4 demonstrate that the mysterious immunity of MIROs to the sense of circular polarization reported previously [13] is not a general feature and could be a property of particular semiconductor samples. This is also supported by the fact that a weak dependence of MIROs on the radiation helicity observed for Corbino disks [14] disappears in some samples. Therefore, it is reasonable to discuss the main distinctions between a 2D electron gas on liquid helium and semiconductor electrons.

Electrons on liquid helium are not immersed in any solid matter; therefore, in the absence of a magnetic field, they have a 2D parabolic spectrum with the free electron mass. For surface electrons, typical relaxation rates and collision broadening of Landau levels are substantially smaller than in semiconductor devices. These properties make electrons on liquid helium an excellent model system for testing theories. Regarding our experiments, the electron density used here is lower by 5–6 orders of magnitude than in semiconductors [13,14], which greatly reduces the superradiant decay rate considered [14] to be a reason for a reduction of $\Delta\sigma_{xx}^{(+)}/\Delta\sigma_{xx}^{(-)}$. As an additional important distinction, we note a contactless method of measurement employed in this work which allows us to exclude completely the influence of near-contact regions.

In summary, by irradiating a nondegenerate 2D electron gas formed on liquid ^{3}He with MWs of different polarizations, we discovered a strong dependence of MIROs on the MW circular polarization direction. This allowed us to report the first observation of the effect of radiation helicity, which provides crucial information for understanding the origin of MW-induced magnetoconductivity oscillations in a 2D electron gas. In particular, our experiments unambiguously support theoretical mechanisms of MIROs based on photon-assisted scattering off disorder.

This work is supported by an internal grant from Okinawa Institute of Science and Technology (OIST) Graduate University. We are grateful to V. P. Dvornichenko for providing technical support.

*denis@oist.jp

[1] M. A. Zudov, R. R. Du, J. A. Simmons, and J. L. Reno, Phys. Rev. B **64**, 201311 (2001).
[2] P. D. Ye, L. W. Engel, D. C. Tsui, J. A. Simmons, J. R. Wendt, G. A. Vawter, and J. L. Reno, Appl. Phys. Lett. **79**, 2193 (2001).
[3] R. Mani, J. H. Smet, K. von Klitzing, V. Narayanamurti, W. B. Johnson, and V. Umansky, Nature (London) **420**, 646 (2002).
[4] M. A. Zudov, R. R. Du, L. N. Pfeiffer, and K. W. West, Phys. Rev. Lett. **90**, 046807 (2003).
[5] M. A. Zudov, O. A. Mironov, Q. A. Ebner, P. D. Martin, Q. Shi, and D. R. Leadley, Phys. Rev. B **89**, 125401 (2014).
[6] D. F. Karcher, A. V. Shchepetilnikov, Yu. A. Nefyodov, J. Falson, I. A. Dmitriev, Y. Kozuka, D. Maryenko, A. Tsukazaki, S. I. Dorozhkin, I. V. Kukushkin, M. Kawasaki, and J. H. Smet, Phys. Rev. B **93**, 041410(R) (2016).
[7] R. Yamashiro, L. V. Abdurakhimov, A. O. Badrutdinov, Yu. P. Monarkha, and D. Konstantinov, Phys. Rev. Lett. **115**, 256802 (2015).
[8] I. A. Dmitriev, A. D. Mirlin, D. G. Polyakov, and M. A. Zudov, Rev. Mod. Phys. **84**, 1709 (2012).
[9] V. I. Ryzhii, Fiz. Tverd. Tela (Leningrad) **11**, 2577 (1969) [Sov. Phys. Solid State **11**, 2078 (1970)].
[10] A. C. Durst, S. Sachdev, N. Read, and S. M. Girvin, Phys. Rev. Lett. **91**, 086803 (2003).
[11] I. A. Dmitriev, A. D. Mirlin, and D. G. Polyakov, Phys. Rev. Lett. **91**, 226802 (2003).
[12] I. A. Dmitriev, M. G. Vavilov, I. L. Aleiner, A. D. Mirlin, and D. G. Polyakov, Phys. Rev. B **71**, 115316 (2005).
[13] J. H. Smet, B. Gorshunov, C. Jiang, L. Pfeiffer, K. West, V. Umansky, M. Dressel, R. Meisels, F. Kuchar, and K. von Klitzing, Phys. Rev. Lett. **95**, 116804 (2005).
[14] T. Herrmann, I. A. Dmitriev, D. A. Kozlov, M. Schneider, B. Jentzsch, Z. D. Kvon, P. Olbrich, V. V. Bel'kov, A. Bayer, D. Schuh, D. Bougeard, T. Kuczmik, M. Oltscher, D.Weiss, and S. D. Ganichev, Phys. Rev. B **94**, 081301(R) (2016).
[15] Yu. P. Monarkha, Fiz. Nizk. Temp. **43**, 819 (2017) [Low Temp. Phys. **43**, 650 (2017)].
[16] S. I. Dorozhkin, A. A. Kapustin, V. Umansky, K. von Klitzing, and J. H. Smet, Phys. Rev. Lett. **117**, 176801 (2016).
[17] *Two-Dimensional Electron System on Helium and other Cryogenic Substrates*, edited by E. Y. Andrei (Kluwer Academic Publishers, Dordrecht, 1997).
[18] Yu. P. Monarkha and K. Kono, *Two-Dimensional Coulomb Liquids and Solids* (Springer-Verlag, Berlin, 2004).
[19] H. Kogelnik and T. Li, Appl. Opt. **5**, 1550 (1966).
[20] L. V. Abdurakhimov, R. Yamashiro, A. O. Badrutdinov, and D. Konstantinov, Phys. Rev. Lett. **117**, 056803 (2016).
[21] K. Park, Phys. Rev. B **69**, 201301(R) (2004).
[22] M. G. Vavilov and I. L. Aleiner, Phys. Rev. B **69**, 035303 (2004).
[23] M. Torres and A. Kunold, Phys. Rev. B **71**, 115313 (2005).
[24] M. I. Dykman and L. S. Khazan, Zh. Eksp. Teor. Fiz. **77**, 1488 (1979) [Sov. Phys. JETP **50**, 747 (1979)].